Hyperosmotically Induced Volume Change and Calcium Signaling in Intervertebral Disk Cells: The Role of the Actin Cytoskeleton

Scott Pritchard,*† Geoffrey R. Erickson,*† and Farshid Guilak*†‡
Departments of *Surgery, †Biomedical Engineering, and ‡Mechanical Engineering and Materials Science, Duke University Medical Center, Durham, North Carolina 27710 USA

ABSTRACT Loading of the spine alters the osmotic environment in the intervertebral disk (IVD) as interstitial water is expressed from the tissue. Cells from the three zones of the IVD, the anulus fibrosus (AF), transition zone (TZ), and nucleus pulposus (NP), respond to osmotic stress with altered biosynthesis through a pathway that may involve calcium (Ca^{2+}) as a second messenger. We examined the hypothesis that IVD cells respond to hyperosmotic stress by increasing the concentration of intracellular calcium ($[Ca^{2+}]_i$) through a mechanism involving F-actin. In response to hyperosmotic stress, control cells from all zones decreased in volume and cells from the AF and TZ exhibited $[Ca^{2+}]_i$ transients, while cells from the NP did not. Extracellular Ca^{2+} was necessary to initiate $[Ca^{2+}]_i$ transients. Stabilization of F-actin with phalloidin prevented the Ca^{2+} response in AF and TZ cells and decreased the rate of volume change in cells from all zones, coupled with an increase in the elastic moduli and apparent viscosity. Conversely, actin breakdown with cytochalasin D facilitated Ca^{2+} signaling while decreasing the elastic moduli and apparent viscosity for NP cells. These results suggest that hyperosmotic stress induces volume change in IVD cells and may initiate $[Ca^{2+}]_i$ transients through an actin-dependent mechanism.

INTRODUCTION

The intervertebral disk (IVD) is a heterogeneous structure comprising three distinct tissue regions including the anulus fibrosus (AF), transition zone (TZ), and the nucleus pulposus (NP) (Fig. 1). The IVD is populated by chondrocyte-like or fibrochondrocyte-like cells of mesenchymal origin in all three zones as well as larger, highly vacuolated cells derived from the notochord that are present only in the NP (Buckwalter, 1995; Maldonado and Oegema, 1992; Oegema, 1993; Trout et al., 1982). These cells are responsible for the synthesis of the IVD matrix during development and maintenance of the extracellular matrix throughout life. Significant zonal variations exist in the phenotypic expression and biosynthetic activity of the IVD, and may reflect the activities of a heterogeneous cell population (Baer et al., 2001; Maldonado and Oegema, 1992; Ohshima et al., 1995; Wang et al., 2001). With increasing age, the notochordal cells are no longer found and changes are observed in the biosynthetic activity of the IVD, particularly in the NP (Antoniou et al., 1996; Buckwalter, 1995; Trout et al., 1982). Age-related changes in cellular phenotype and biosynthesis are hypothesized to impair the intrinsic ability of the IVD to maintain and repair its extracellular matrix, and therefore may be involved in the progressive development of disk degeneration (Buckwalter, 1995; Oegema, 1993).

Under normal physiologic conditions, the IVD is subjected to dynamic compressive loads that lead to diurnal variations in disk height and water content (McMillan et al., 1996; Paajanen et al., 1994). IVD cells have been shown to respond to static or oscillatory compressive loading in a non-uniform and dose-dependent manner (Colliou et al., 1998; Ishihara et al., 1992; Ohshima et al., 1995; Toribatake et al., 1997). For example, compressive loads applied to the motion segment in vivo have been associated with altered proteoglycan synthesis in the NP and altered collagen biosynthesis in the AF (Colliou et al., 1998; Toribatake et al., 1997). Higher compressive loads applied to motion segments in vitro have been shown to inhibit proteoglycan or collagen synthesis in all cells of the IVD, while higher frequencies of oscillation have been shown to inhibit proteoglycan synthesis in the NP cells alone (Ishihara et al., 1992; Ohshima et al., 1995). The biophysical mechanisms involved in mechanical signal transduction by IVD cells are not fully understood, but are believed to involve changes in the interstitial osmolality or pH secondary to exudation of interstitial water (Malko et al., 1999; Ohshima et al., 1989; Paajanen et al., 1994). With compression, an increase in the interstitial fixed charge density attracts more counterions into the tissue, resulting in a hyperosmotic extracellular environment (Ishihara et al., 1997; Urban et al., 1994). As the cell membrane is relatively permeable to water, increasing the extracellular osmolality leads to a decrease in cell volume (Verkman et al., 1996). In some cell types, alterations in cell volume are responsible for triggering various volume recovery mechanisms that involve the activation of ion channels and the initiation of intracellular signaling cascades in an effort to restore cell volume (Erickson and Guilak, 2001; Guizouarn et al., 2000; Hoffmann and Dunham, 1995; Lange, 2000; O'Neill, 1999; Perlman and Goldstein, 1999; Waldegger et al., 1998). In particular, the concentration of intracellular calcium ion ($[Ca^{2+}]_i$) is believed to play a role in regulatory volume control (McCarty and O'Neil, 1992) and has been shown to increase in certain

Submitted January 18, 2002, and accepted for publication June 3, 2002.
Address reprint requests to Farshid Guilak, Ph.D., Orthopaedic Research Laboratories, Duke University Medical Center, 375 Medical Sciences Research Building, Research Drive, Box 3093, Durham, NC 27710. Tel.: 919-684-2521; Fax: 919-681-8490; E-mail: guilak@duke.edu.

0006-3495/02/11/2502/09 $2.00

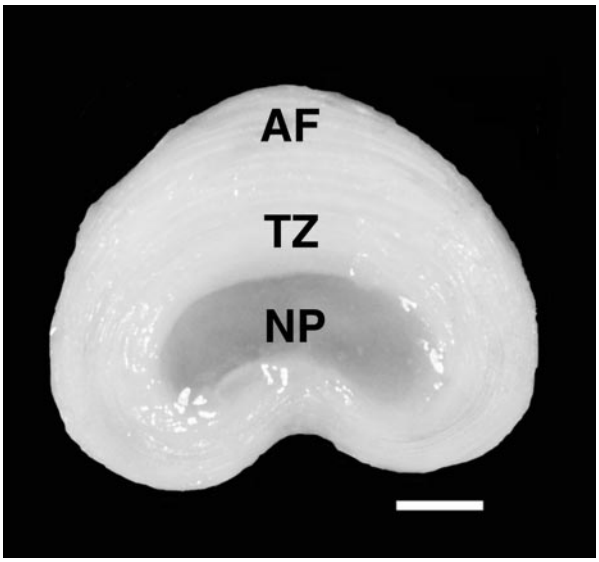

FIGURE 1 Cross-section of a porcine intervertebral disk. The anulus fibrosus (AF) lies at the disk periphery, while the nucleus pulposus (NP) occupies the central portion of the disk. The transition zone (TZ) lies between these two tissues. Scale bar = 1 cm.

cells in response to osmotic stress (Lang et al., 1998). Of relevance to the process of mechanical signal transduction is that cell volume recovery, which includes the influx and efflux of various solutes, can lead to the activation of intracellular signaling cascades (Banuett, 1998; Ragette et al., 1997; Schliess et al., 1996; Warskulat et al., 1998) such as transient or oscillatory changes in $[Ca^{2+}]_i$ (McCarty and O'Neil, 1992). These cascades may not necessarily be involved in only the volume regulation process, but may also influence other cellular responses such as gene expression, cellular metabolism, and apoptosis (Asada et al., 2001; Dascalu et al., 1996, 2000; Hardingham and Bading, 1999; Hildebrandt and Prowald, 2000; Schliess et al., 1996).

An important morphologic difference that has been identified between cells of the NP and those of the AF or TZ is the abundant distribution of cytoplasmic actin filaments in NP cells (Guilak et al., 1999; Maldonado and Oegema, 1992; Trout et al., 1982). The actin network plays a dominant role in the mechanical behavior of many cell types (Guilak et al., 1999; Ingber et al., 1994; Sheikh et al., 1997; Small and Gimona, 1998; Trickey et al., 2000; Tseng et al., 2001; Wang, 1998) and is likely to play an important role in the cellular response to osmotic stress (Kajstura and Reiss, 1989; Rivero et al., 1996; Ting-Beall et al., 1995; Tsai et al., 1994). This hypothesis is supported by several studies that suggest a role for the actin cytoskeleton in cell volume regulation and the initiation of $[Ca^{2+}]_i$ transients (Cantiello, 1997; Hallows et al., 1996; Henson, 1999; Maximov et al., 1997; Moustakas et al., 1998; Rosado and Sage, 2000). Recent work has identified actin itself as a potential source of $[Ca^{2+}]_i$, as significant stores of Ca^{2+} are bound in the actin cytoskeleton and may be released in the cytoplasm in the event of actin depolymerization (Al Mohanna et al., 1997; Lange and Brandt, 1996). The zonal differences in the organization of the actin cytoskeleton and mechanical properties of IVD cells (Guilak et al., 1999) suggest that cells of the AF and TZ may respond differently than those of the NP.

The objective of this study was to examine the hypothesis that hyperosmotic stress initiates a transient increase in $[Ca^{2+}]_i$ in cells of the IVD, and to determine whether differences exist in these $[Ca^{2+}]_i$ transients and volume change among cells of the AF, TZ, and NP. Furthermore, the role of the actin cytoskeleton in osmotically induced volume adaptation, $[Ca^{2+}]_i$ signaling, and cellular mechanical properties was examined by either disrupting or stabilizing F-actin.

MATERIALS AND METHODS

Cell culture

Unless otherwise noted, reagents and chemicals were obtained from Gibco-BRL (Grand Island, NY). IVD tissue was harvested from the lumbar spine of 4–5-month-old pigs ($N = 7$) obtained from a local abattoir. For each pig, the AF, TZ, and NP were dissected separately from six lumbar disks, pooled by zone, and stored at room temperature in wash medium containing DMEM-high glucose, supplemented with 100 μg/ml kanamycin (Sigma Chemical, St. Louis, MO), 150 μg/ml gentamicin, and 1 μg/ml fungizone. The tissue was minced and cultured overnight in wash medium supplemented with 5% fetal bovine serum (317 mOsm) in a humidified atmosphere at 37°C and 5% CO_2. Cells were isolated from the tissue by a sequential pronase/collagenase digestion modified from a previously published protocol (Maldonado and Oegema, 1992). The tissue was digested for 90 min in 0.2% pronase followed by an overnight digestion in 0.15% collagenase. After digestion, isolated cell suspensions were filtered through a 70 μm nylon mesh filter (Falcon Cell Strainer; Becton Dickinson, Franklin Lakes, NJ) to remove debris. The cell pellet was then washed by sequential rinsing and centrifugation at 400 $\times$ g for 10 min. Cell viability was determined using a trypan blue exclusion assay and viability was found to be >95% in all cases. The cells were plated at a density of 1.5 million cells/ml on 31 mm glass coverslips (no. 1.5, VWR Scientific, West Chester, PA) in six well culture plates. The coverslips were pretreated with sterile poly-L-lysine (Sigma Chemical) to improve cell adhesion to the glass. The cells were allowed to adhere for 45 min and then each well was filled with 2 ml of feed medium (DMEM-F12 + 10% FBS) without antibiotics. The cells were cultured overnight at 37°C to reach stability for testing. All tests were performed between 12 and 24 h after the cells were isolated and plated on glass to ensure that the cells maintained a rounded morphology for testing.

Alteration of the actin cytoskeleton

To alter the actin microfilament network, IVD cells from the three zones were treated with 2 μM cytochalasin D to disrupt F-actin (Schliwa, 1982), or 1 μM phalloidin (Molecular Probes, Inc., Eugene, OR) which binds and stabilizes F-actin (Kinosian et al., 1993; Le Bihan and Gicquaud, 1991; Wendel and Dancker, 1987). Experiments were performed after the cells had been exposed to the pharmacological reagents for 3 h.

The effect of cytochalasin D or phalloidin was qualitatively assessed by immunofluorescence microscopy. Control and treated cells from the three zones were plated overnight on LabTek chambered slides (Nalge Nunc

International, Naperville, IL) pretreated with sterile poly-L-lysine (Sigma Chemical). The cells were fixed in 3.7% formaldehyde (in PBS) for 15 min, washed twice with PBS, and permeabilized with 0.1% Triton X-100 in PBS for 5 min. After washing twice with PBS for 10 min, a blocking solution of 1% BSA in PBS was applied for 30 min, followed by application of a primary antibody to actin (JLA-20, 1:10 dilution in PBS, developed by Alice B. Fulton and obtained from the Developmental Studies Hybridoma Bank, University of Iowa, Iowa City, IA) in blocking solution for 1 h. Cells were washed three times with PBS for 10 min, and a fluorescent secondary antibody (Alexa-Fluor 488 anti-mouse, 1:50 dilution in PBS, Molecular Probes) was applied for 30 min. Finally, a coverslip was applied using mounting media consisting of a 1:1 mixture of glycerol and PBS. Fluorescent images were recorded on a confocal microscope with excitation of 488 nm (argon ion laser) and emission recorded at 525 nm using a 1.2 NA, 63× water immersion objective lens (LSM 510, Zeiss, Thornwood, NY).

Osmotic stress

Coverslips with adherent cells were mounted in a custom-built heated perfusion chamber containing isosmotic media (DMEM/F12–310 mOsm). All experiments were performed at 37°C. A control experiment was performed for each group, in which cells were perfused with isosmotic media. Cells were perfused with hyperosmotic media consisting of DMEM/F12 adjusted to 450 mOsm by the addition of either sodium chloride (NaCl) or sucrose. It was found that the volumetric response to hyperosmotic stress was independent of the solute used to adjust the media osmolality. AF cells shrank to a final volume of 0.80 (normalized to initial volume) after exposure to the hyperosmotic sucrose solution, and 0.81 after exposure to the hyperosmotic NaCl solution. The rate of volume decrease (time constant) was the same for both solutes (122 s vs. 127 s for NaCl and sucrose, respectively). To avoid disruption of the transmembrane sodium and chloride gradients, sucrose was used in the preparation of hyperosmotic media for all experiments. The osmolality of the solutions was measured using a freezing point osmometer (Osmette 2007, Precision System Inc., Natick, MA). The perfusion was carried out by drawing the isosmotic media out of the chamber through a syringe and perfusing with hyperosmotic media through a second syringe mounted on the opposite side of the chamber. The exchange of medium was performed in ~3 s.

Calcium-free experiments

Hyperosmotic media without Ca^{2+} was prepared by adding 1 M sterile sucrose to the calcium-free (Ca^{2+}-free) isosmotic solution (DMEM/F12) and media osmolality was measured on a freezing point osmometer (Osmette 2007, Precision Systems). Cellular response to osmotic stress was tested as described above, after the cells were washed briefly with the isosmotic Ca^{2+}-free media.

Calcium imaging

Laser scanning microscopy was used to measure changes in $[Ca^{2+}]_i$. Cells were loaded, before testing, with two visible light fluorescent Ca^{2+} indicators: Fura-Red AM (20 μM) and Fluo-3 AM (15 μM) (Molecular Probes, Inc.) for 20 min. $[Ca^{2+}]_i$ transients were measured using a previously described ratio imaging technique on a confocal laser scanning microscope (LSM 510, Zeiss) (Lipp and Niggli, 1993) using a 63×, 1.2 NA water immersion objective lens (Zeiss). The sample was excited using an argon ion laser (488 nm) and fluorescence emission was recorded at 505–550 nm (Fluo-3) and at greater than 650 nm (Fura-Red). Images were recorded at a scan rate of 0.33 Hz for 11 min to track relative $[Ca^{2+}]_i$. The fluorescence intensity of Fluo-3 was divided by the fluorescence intensity of Fura-Red. The use of a ratiometric approach serves to amplify the fluorescent signal, and corrects for focal changes over the course of the test. An increase of 10% above baseline of the intensity ratio was considered to represent a positive $[Ca^{2+}]_i$ response. A positive control was carried out for all cells by treatment at 600 s with 10 μM ionomycin to confirm that the cells were viable and that $[Ca^{2+}]_i$ stores were functional and had not been depleted.

Measurement of cell volume

Cell volume was measured from differential interference contrast (DIC) images collected on the laser scanning microscope. Images were obtained over time at a scan rate of 0.10 Hz for 20 min. The projected surface area of the cells (in square pixels) was measured using an edge-detection algorithm and cell volume was calculated assuming a spherical morphology (Alexopoulos et al., 2002). The time constant (τ) describing the transient change in cell volume was determined using a nonlinear regression of the data to the following exponential model:

$$V = 1 - (1 - V_f)(1 - e^{-t/\tau}) \quad (1)$$

where V is the volume, V_f is the final volume, t is the time, and τ is the time constant of volume change. The value of τ was reported for each cell.

Micropipette aspiration and mechanical testing

Micropipette aspiration was performed using techniques we have described previously (Jones et al., 1999). Micropipettes were custom-made by drawing 70 μm capillary tubes (A-M Systems, Carlsborg, WA) with a pipette puller (David Kopf Instruments, Tujunga, CA) and fracturing them on a microforge to an inner diameter of 6–13 μm to achieve a cell-to-pipette ratio of >1.5:1. The micropipettes were coated with Sigmacote (Sigma Chemical) to prevent cell adhesion during testing.

Isolated cells were suspended at $\sim 5 \times 10^4$ cells/ml in 0.9% (w/v) NaCl containing 0.1% BSA. A chamber that allowed side entry of the pipette was filled with 700 μl of cell suspension. A glass coverslip (no. 1 thickness) was used as the bottom of the chamber to provide a short, optically clear path between the objective lens and the cells. All experiments were performed at room temperature within 24 h of cell isolation.

A custom-built adjustable water reservoir was used to apply a pressure gradient to the cell surface. Pressures were measured directly with an in-line pressure transducer with a resolution of 1 Pa (model no. DP15–28, Validyne Engineering Corp., Northridge, CA). During the experiment, video images of cell aspiration into the micropipette were captured at 60 fields/s with a CCD camera (COHU, San Diego, CA) through a bright-field microscope (Nikon, Melville, NY), using a 60× (1.4 NA) or 40× (1.3 NA) oil immersion objective lens (Nikon) and a 10× or 5× wide-field eyepiece (Edmund Scientific, Barrington, NJ). The applied pressure and time were displayed on the monitor by a digital multiplexer (Vista Electronics, Ramona, CA). The length of cell aspiration into the pipette was measured using a custom image analysis program written in Matlab (The MathWorks Inc., Natick, MA) which was verified against a previously described technique (video calipers) (Jones et al., 1999). The initial diameter of each cell was obtained before testing by averaging the horizontal and vertical diameters. The micropipette diameter was also measured, and the value multiplied by a factor of 0.92. This factor adjusts for the micropipette lens artifact due to the differences in refractive indices between the micropipette glass and surrounding solution and for the focusing error due to diffraction phenomena (Engstrom et al., 1992; Jones et al., 1999).

The experiment was initiated by applying a tare pressure of 10 Pa to the cell surface for 30 s to achieve an initial test geometry and to ensure a complete pressure seal. A test pressure (Δp) of 100–450 Pa was then applied to the cell, and images of cell aspiration into the micropipette were recorded for a period of 300 s, or until an equilibrium conformation was achieved.

The viscoelastic mechanical properties of the cell were determined from recorded pressure and aspiration length data using a theoretical model of the cell as an axisymmetric homogeneous half-space subjected to a uniform applied pressure on its surface (Sato et al., 1990). A three-parameter viscoelastic model (standard linear solid) was used to represent the material behavior of the cell under conditions of small deformation and assuming intrinsic incompressibility of the cell. The governing equations for this model were solved subject to the boundary conditions of a uniform, axisymmetric pressure applied over the interface with the micropipette and of no axial displacement of the cell at the micropipette end. The solution for cell displacement L at time t is governed by the parallel and series elastic parameters (k_1 and k_2, respectively), the apparent viscosity (μ), the characteristic time constant (τ_1), the applied pressure (Δp), and the inner (a) and outer (b) radii of the micropipette. For this "rigid punch" model, a dimensionless parameter (Φ) was used to incorporate the effect of wall thickness for the micropipette. A value of 2.1 was used for the entire range of values of a and b in this study. The values for k_1, k_2, τ_1, and μ were determined by nonlinear regression of the experimental data to the following equations:

$$L(t) = \frac{\Phi a \Delta p}{\pi k_1}\left[1 - \frac{k_2}{k_1 + k_2}\, e^{-t/\tau_1}\right] \tag{2}$$

$$\mu = \frac{\tau_1 k_1 k_2}{k_1 + k_2} \tag{3}$$

Statistical analysis

The percentage of cells responding with a significant increase in $[Ca^{2+}]_i$ is reported for each test condition. Comparisons among the different conditions were made by chi-square analysis using a commercially available software package (StatView, SAS Institute Inc., Cary, NC). All other data are presented as mean ± one standard deviation and statistical analysis was performed using a one-factor or two-factor ANOVA followed by Fisher's PLSD post hoc test (StatView). Significance was reported at the 95% confidence level.

RESULTS

Alteration of the actin network

Untreated cells from the AF and TZ showed a cortical localization of actin as visualized by immunofluorescent labeling (Fig. 2, *A* and *B*). Cells from the NP displayed an abundant actin network that was more disperse than in the AF and TZ cells, with filaments extending from the cortical region into the cytoplasm (Fig. 2 *C*). Pretreatment with cytochalasin D resulted in a disruption of the organized actin network seen in untreated cells (Fig. 2, *D–F*), while pretreatment with phalloidin resulted in an increase in actin organization and density in all three cell types (Fig. 2, *G–I*).

Calcium signaling and osmotic stress

Control experiments indicated that replacement of the isosmotic media with an identical solution did not change $[Ca^{2+}]_i$ in any of the cells tested. Exposure of the cells to hyperosmotic media led to either a transient increase in $[Ca^{2+}]_i$ or a stable baseline level of $[Ca^{2+}]_i$ (Fig. 3). The transients were characterized by a sharp rise in $[Ca^{2+}]_i$ followed by a return to baseline levels (Fig. 3). All tested cells (untreated and treated) were viable as they responded to ionomycin treatment by releasing Ca^{2+} from intracellular stores.

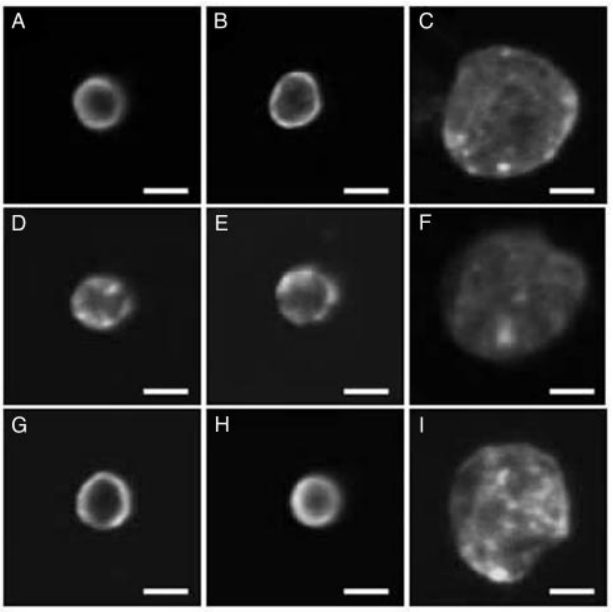

FIGURE 2 Actin structure visualized by laser microscopy using a primary antibody to actin, and a fluorescent secondary antibody. (*A–C*) Untreated cells from the AF, TZ, and NP. (*D–F*) Cells from the AF, TZ, and NP after 3 h treatment with 2 μM cytochalasin D. (*G–I*) Cells from the AF, TZ, and NP after 3 h treatment with 1 μM phalloidin. Scale bar = 10 μm.

The percentage of AF and TZ cells that responded to hyperosmotic stress by increasing $[Ca^{2+}]_i$ was significantly greater than the isosmotic control (59.1% and 69.2% vs. 0%, Table 1). The percentage of NP cells that displayed a transient increase in $[Ca^{2+}]_i$ was not significantly different

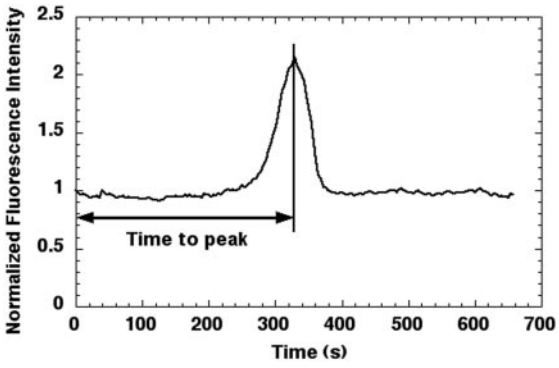

FIGURE 3 Representative trace of $[Ca^{2+}]_i$ over time after hyperosmotic stimulation. This trace shows the response of an untreated AF cell after exposure to 450 mOsm media. This $[Ca^{2+}]_i$ profile was typical for responsive cells. The vertical axis represents the ratio of Fluo-3 intensity to Fura Red intensity normalized to the value at time $t = 0$. The time to reach a peak $[Ca^{2+}]_i$ was recorded for all responsive cells.

TABLE 1 The percentage of cells in each group that responded with a transient increase in $[Ca^{2+}]_i$ (defined as increase of 10% over baseline) after hyperosmotic stress

	310 mOsm	Untreated	Cyt D	Phalloidin	Ca^{2+}-Free
AF	0	59.1*	60.0	0**	4**
TZ	0	69.2*	72.2	0**	0**
NP	0	8.7***	36.8**	0	—

*$p < 0.001$ vs. 310 mOsm control; **$p < 0.001$ vs. untreated group of same cell type; ***$p < 0.001$ vs. AF/TZ untreated (n = 15–30 cells per group, two to three independent experiments per group, Chi-squared test).

from the isosmotic control (8.7% vs. 0%, Table 1). Pretreatment with cytochalasin D did not affect the percentage of AF and TZ cells that responded (60.0% and 72.2%, Table 1), while the percentage of NP cells responding to hyperosmotic stress increased significantly (36.8%, Table 1) after cytochalasin D pretreatment. Cells from all three tissue zones pretreated with phalloidin did not generate $[Ca^{2+}]_i$ transients (Table 1). The time-to-peak $[Ca^{2+}]_i$ was not significantly different between untreated cells and those pretreated with cytochalasin D (340.9 ± 100.3 vs. 320.7 ± 102.2 s), and no difference was observed among the three tissue zones.

To determine whether the Ca^{2+} mobilized by the cells during the initiation of intracellular transients required the presence of extracellular Ca^{2+}, cells were exposed to hyperosmotic stress in Ca^{2+}-free media. Control experiments confirmed that an exposure to isosmotic Ca^{2+}-free media did not elicit an increase in $[Ca^{2+}]_i$, and that the presence of Ca^{2+}-free media did not deplete the $[Ca^{2+}]_i$ stores over the time of testing (positive response to ionomycin treatment at 600 s). Upon perfusion with hyperosmotic Ca^{2+}-free media, only 4% of AF cells showed an increase in $[Ca^{2+}]_i$ (Table 1) and none of the TZ cells responded to the hyperosmotic stimulus.

Cell volume change and osmotic stress

Control experiments confirmed that no volume change occurred following perfusion of cells with isosmotic media. In response to hyperosmotic stress, cells from all three of the tissue zones significantly decreased in volume under all conditions. The extent of volume decrease (normalized final volume) was the same for untreated cells from each of the three zones over the 20 min test period (0.78–0.80). When pretreated with cytochalasin D, the cells from the NP decreased in volume to a greater degree than the untreated NP cells (0.65 ± 0.01 vs. 0.78 ± 0.04). Cytochalasin D pretreatment did not affect the extent of volume change in cells from the AF and TZ as compared to untreated control (0.79–0.80). Pretreatment with phalloidin had no significant effect on the extent of volume change in any of the three cell types (0.78–0.81)

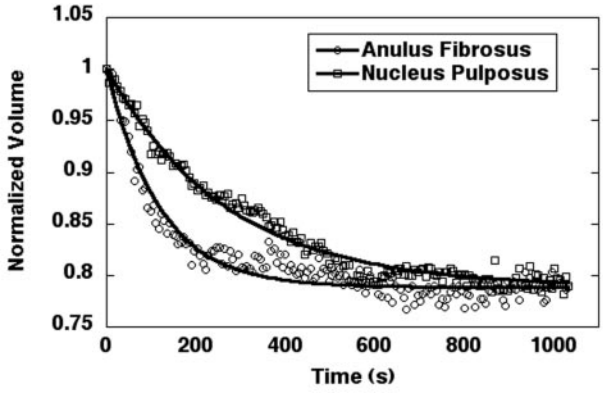

FIGURE 4 Sample nonlinear regression of the volume data. The individual data points represent the experimental results, while the solid line shows the exponential curve fit to Eq. 1. The data shown are for an untreated AF and NP cell after hyperosmotic stimulation (τ = 117.3 and 268.2, respectively. $R^2 > 0.94$).

To quantify the rate of change of cell volume, the experimental volume data were fit to an exponential curve, and a time constant for cell volume change (τ) was determined (Fig. 4). The correlation coefficient (R^2) was >0.9 in all cases. The time constant for volume decrease was significantly higher in untreated NP cells than in untreated cells from the AF and TZ (Fig. 5). After pretreatment with phalloidin, τ increased significantly for cells from all three zones (Fig. 5), and experiments in this case were carried out for 1 h to ensure that the cells had reached an equilibrium volume. Pretreatment with cytochalasin D had no significant effect on τ for cells from the AF and TZ, but resulted in a significant decrease in τ for cells from the NP (Fig. 5).

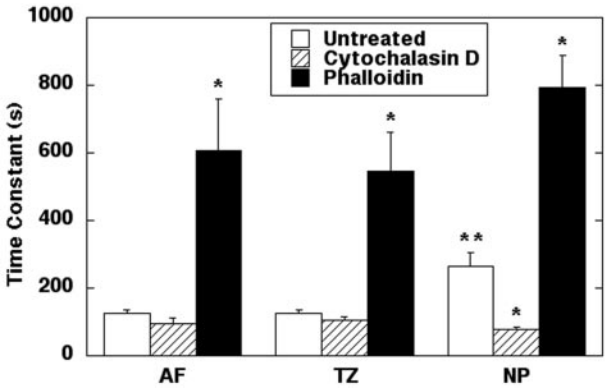

FIGURE 5 Time constant (τ) for cell volume decrease determined from nonlinear regression of the experimental data. Untreated NP cells displayed a higher time constant than AF/TZ cells. Treatment with phalloidin resulted in an increase in the time constant relative to the untreated group in all cell types. Cytochalasin D decreased the time constant only in NP cells. *$p < 0.001$ vs. untreated group of same cell type, **$p < 0.01$ vs. AF/TZ untreated (n = 10 cells per group, ANOVA and Fisher's PLSD). Data are presented as mean ± SD.

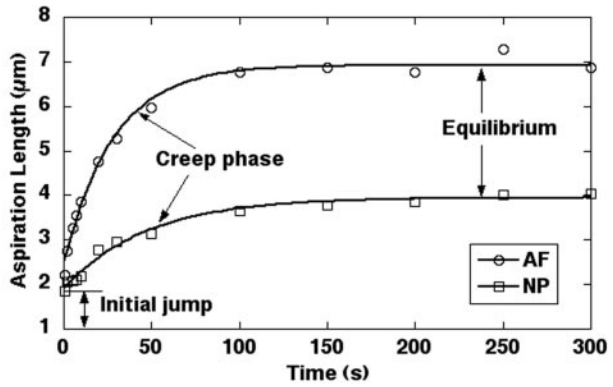

FIGURE 6 Viscoelastic creep behavior of intervertebral disk cells in response to applied pressure. With the application of a step increase in pressure, cell behavior was characterized by an initial jump of the cell surface into the micropipette followed by an asymptotic approach to an equilibrium length. Cell properties in these representative examples were as follows: anulus fibrosus (AF): $k_1 = 103$ Pa, $k_2 = 147$ Pa, and $\mu = 2095$ Pa-s; nucleus pulposus (NP): $k_1 = 197$ Pa, $k_2 = 142$ Pa, and $\mu = 5105$ Pa-s. Data points indicate experimental measurements, while lines indicate the model fit ($R^2 = 0.98$ for these cases). The longer creep time and smaller equilibrium displacement of the NP cell as compared to the AF cell in this example are characteristic of the typical response.

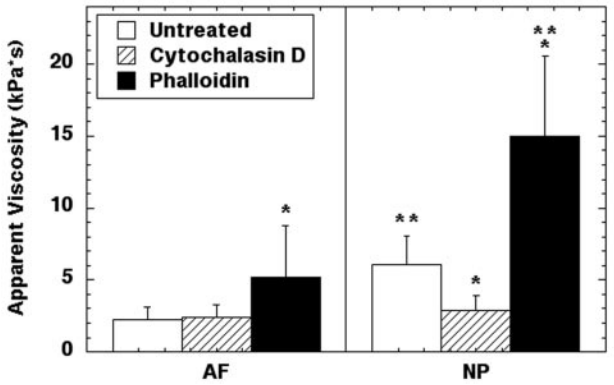

FIGURE 8 Apparent viscosity (μ) of cells from the anulus fibrosus (AF) and nucleus pulposus (NP) before and after treatment with cytochalasin D or phalloidin. *$p < 0.01$ vs. untreated control of same cell type, **$p < 0.01$ vs. same treatment group in AF cells (n = 15–20 cells per group, ANOVA and Fisher's PLSD). Data are presented as mean ± SD.

Mechanical properties of IVD cells

All cells tested exhibited viscoelastic solid behavior, displaying an initial jump into the micropipette followed by a creep displacement to an equilibrium conformation (Fig. 6). Model predictions of this behavior were excellent, with a correlation coefficient for all cells of greater than $R^2 = 0.9$. Untreated cells from the NP showed significantly higher values than AF cells for the instantaneous modulus ($k_1 + k_2$) and equilibrium modulus (k_1) (Fig. 7). In addition, the apparent viscosity (μ) of NP cells was greater than that of cells from the AF (Fig. 8). Treatment of cells with cytochalasin D resulted in a significant decrease in k_1 for both AF and NP cells and a significant decrease in $k_1 + k_2$ and μ for NP cells only (Fig. 7 and Fig. 8). Treatment of cells with phalloidin had the opposite effect and significantly increased k_1, $k_1 + k_2$, and μ in AF cells, and significantly increased $k_1 + k_2$ and μ in NP cells (Figs. 7 and 8).

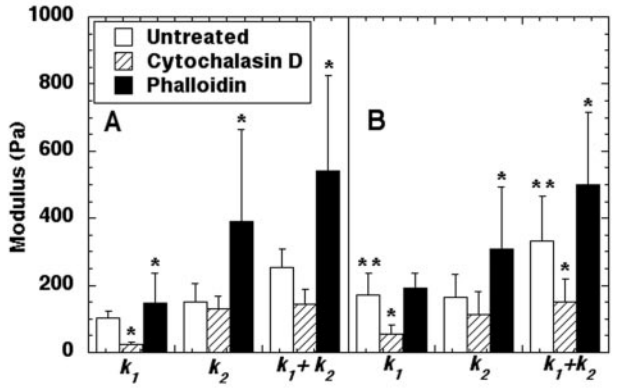

FIGURE 7 Elastic coefficients (k_1, k_2, and $k_1 + k_2$) of cells from anulus fibrosus (AF) and nucleus pulposus (NP) before and after treatment with cytochalasin D or phalloidin. The equilibrium elastic modulus is represented by k_1, and the instantaneous elastic modulus is represented by $k_1 + k_2$. *$p < 0.01$ vs. untreated control of same cell type, **$p < 0.01$ vs. same treatment group in AF cells. (n = 15–20 cells per group, ANOVA and Fisher's PLSD). Data are presented as mean ± SD.

DISCUSSION

The findings of this study indicate that hyperosmotic stress causes a significant decrease in the volume of IVD cells, accompanied by a transient increase in $[Ca^{2+}]_i$ in the majority of untreated cells from the AF and TZ, but not those of the NP. Our results suggest an important role for the actin cytoskeleton in this response, as evidenced by the finding that a stabilized F-actin network inhibited osmotically induced Ca^{2+} mobilization. Furthermore, the integrity of the F-actin organization was shown to influence the viscoelastic properties of the cells and the rate of volume adaptation after hyperosmotic stress. Together, these findings suggest that the actin cytoskeleton may play an important role in the biological response of IVD cells to mechanical compression in situ.

A major finding of this study was the observation that hyperosmotic stress, in the absence of other matrix-related biophysical effects, induced a transient alteration in cellular volume and the $[Ca^{2+}]_i$ in AF and TZ cells, but not in those of the NP. Several of our findings suggest that this response is in part dependent on the integrity and organization of the cytoskeleton, which differs significantly between cells of the NP and those of the AF or TZ (Guilak et al., 1999; Maldonado and Oegema, 1992; Trout et al., 1982). Cells from all three zones that were pretreated with phalloidin to

stabilize the F-actin network (Fig. 1) did not exhibit an increase in $[Ca^{2+}]_i$. Furthermore, hyperosmotic stress induced $[Ca^{2+}]_i$ transients in NP cells that had been treated with cytochalasin D to disrupt the F-actin. Previous studies have shown that remodeling of the actin cytoskeleton is an important step in the cellular response to osmotic stress (Cantiello, 1997; Hallows et al., 1996; Moustakas et al., 1998), and that F-actin may in fact serve as an intracellular store of Ca^{2+} (Al Mohanna et al., 1997; Lange and Brandt, 1996). Furthermore, several recent studies have suggested that the existence of a dense actin network adjacent to the cell membrane may interfere with the diffusion of small molecules and ions (such as Ca^{2+}) into and out of the cell (Lange, 1999). This finding, in light of the fact that extracellular influx of Ca^{2+} was shown to be necessary for calcium signaling in our system, may help to explain the absence of $[Ca^{2+}]_i$ transients after pretreatment with phalloidin.

The mechanism by which IVD cells are able to transduce the applied osmotic stress into a $[Ca^{2+}]_i$ transient is currently unclear. The observed lag between application of hyperosmotic stress (seconds) and influx of $[Ca^{2+}]_i$ (several minutes) suggests that the response is triggered not by the presence of an osmotic gradient, but rather by some downstream cellular response to the osmotic stress. Some possible transducers include one or a combination of the following: cellular volume change, membrane stretch, and membrane depolarization. Further work is required to determine how the cell senses the presence of an osmotic gradient and initiates the generation of $[Ca^{2+}]_i$ transients.

Cells from each of the three tissue zones decreased in volume significantly after exposure to hyperosmotic stress, but exhibited no significant regulatory volume increase over the time of testing either in the presence or absence of $[Ca^{2+}]_i$ transients (Bibby and McCulloch, 1994; Hall et al., 1996; Hamilton et al., 1993). This response differs from that observed in porcine articular chondrocytes, in which the cells actively regulate their volume in a $[Ca^{2+}]_i$-dependent manner and appear to decrease in volume at a faster rate (Erickson et al., 2001; Bush and Hall, 2001). These differences suggest that IVD cells and chondrocytes respond in a distinct manner to the application of hyperosmotic stress, possibly due to intrinsic differences in cell properties or due to differences in their in vivo environment. Within the IVD, zonal variations in the cellular volumetric response to hyperosmotic stress were also observed. The volume adaptation characteristics of NP cells differed markedly from those of AF and TZ cells, also in a manner that was dependent on the integrity of the F-actin network. In addition to differences in the F-actin network, cells from the NP are significantly larger and contain numerous vacuoles, which may play a role in the response to hyperosmotic stress (Guilak et al., 1999). Significant differences in the volumetric response to hyperosmotic stress were also observed in cells from all three tissue zones after treatment with actin-modifying reagents. With cytochalasin D treatment, NP cells exhibited significantly greater decreases in volume than AF or TZ cells. Furthermore, the time constant for volume adaptation (τ) for NP cells was significantly higher that those of AF and TZ cells and was decreased by cytochalasin D treatment. Conversely, phalloidin increased τ in all three cell types. These findings further suggest that the intrinsic microfilament network strongly influences cellular volume adaptation after osmotic stress.

Given the lack of active volume regulation in IVD cells, our findings suggest that the differences in the magnitude and rate of volumetric changes in response to hyperosmotic stress are dependent on the viscoelastic mechanical properties of the cells. This hypothesis is supported by the observation that NP cells are significantly stiffer and more viscous than AF or TZ cells as measured by micropipette aspiration (Guilak et al., 1999). Furthermore, disruption of the actin causes a significant decrease in cell stiffness and apparent viscosity, while actin stabilization has the reverse effect. These results are generally consistent with those observed in other cell types, although no other information is available specifically on IVD cells. In articular chondrocytes, cytochalasin D has been shown to decrease chondrocyte stiffness and viscosity by over 80% (Trickey et al., 2000), and hyposmotic stress of chondrocytes causes a transient dispersion and reorganization of the cortical F-actin of chondrocytes, leading to a decrease in k_1, k_2, and μ (Guilak et al., 2002). Cytochalasin D, on one hand, has also been shown to disrupt F-actin and diminish the micromechanical properties of hepatocytes, neutrophils, and endothelial cells (Sato et al., 1990; Tsai et al., 1994; Wu et al., 2000). Phalloidin, on the other hand, acts to stabilize actin in its filamentous form, particularly at the cell cortex (Fig. 2), and thus it is not surprising that the stiffness and viscosity of the cell are increased (Kinosian et al., 1993; Le Bihan and Gicquaud, 1991; Wendel and Dancker, 1987). Together, these findings suggest that the F-actin cytoskeleton plays an important mechanical role in the cellular response to hyperosmotic stress.

Several factors distinguish the in vitro experiments described here from the in vivo or in situ situation. Although the cells were tested in a rounded morphology, there is significant evidence that cells from all three zones of the IVD (especially the AF) may deviate significantly from this geometry (Errington et al., 1998). The presence of abundant cell-matrix attachments in the tissue leads to a complex 3-D cell geometry and likely has an impact on the cell level strains experienced after exposure to hyperosmotic stress. A rounded morphology was chosen for these studies to ensure a consistent cell geometry and thus allow for meaningful comparison between cells from the three tissue zones. It is also important to note that in situ, the exposure to hyperosmotic stress upon loading does not occur instantaneously as in this study. A gradual increase in the osmolality of the surrounding interstitial fluid would be expected to decrease

the rate of cellular volume decrease. The cells used in this study were isolated from the tissue into wash media at an osmolality of ~317 mOsm. Due to the fixed-charge density of the extracellular matrix, the native tissue osmolality is estimated to be higher than this value (400–450 mOsm) (Ishihara et al., 1997), suggesting that the cells swell significantly upon isolation from the tissue. However, following overnight culture, the cells were observed to equilibrate at a stable volume. Our findings therefore suggest that the change in media osmolality is a relevant stimulus, independent of the absolute osmolality.

In conclusion, this work provides evidence that isolated cells from the AF or TZ of the IVD respond to hyperosmotic stress by initiating transient increases in $[Ca^{2+}]_i$ through an actin-dependent mechanism. Previous studies have shown that changes in the osmotic environment alter the biosynthetic response of IVD cells, potentially serving as a regulator of disk metabolism in both health and disease (Ishihara et al., 1997). It remains to be determined what role Ca^{2+} plays as a signaling second messenger in the generation of biosynthetic changes downstream of hyperosmotic stress.

We thank Dr. Lori Setton for many helpful discussions. We also thank Leonidas Alexopoulos for providing assistance with image analysis and James Grant for assistance with the data analysis.

This work was supported by National Institutes of Health Grants AR43876, AG15768, AR047442, and GM08555.

REFERENCES

Alexopoulos, L., G. Erickson, and F. Guilak. 2002. A method for quantifying cell size from differential interference contract (DIC) images: validation and application to osmotically stressed chondrocytes. *J. Microsc.* 205:125–135.

Al Mohanna, F. A., E. J. Pettit, and M. B. Hallett. 1997. Does actin polymerization status modulate Ca^{2+} storage in human neutrophils? Release and coalescence of Ca^{2+} stores by cytochalasins. *Exp. Cell Res.* 234:379–387.

Antoniou, J., T. Steffen, F. Nelson, N. Winterbottom, A. P. Hollander, R. A. Poole, M. Aebi, and M. Alini. 1996. The human lumbar intervertebral disk: evidence for changes in the biosynthesis and denaturation of the extracellular matrix with growth, maturation, aging, and degeneration. *J. Clin. Invest.* 98:996–1003.

Asada, S., K. Fukuda, F. Nishisaka, M. Matsukawa, and C. Hamanisi. 2001. Hydrogen peroxide induces apoptosis of chondrocytes; involvement of calcium ion and extracellular signal-regulated protein kinase. *Inflamm. Res.* 50:19–23.

Baer, A. E., J. Y. Wang, V. B. Kraus, and L. A. Setton. 2001. Collagen gene expression and mechanical properties of intervertebral disk cell-alginate cultures. *J. Orthop. Res.* 19:2–10.

Banuett, F. 1998. Signaling in the yeasts: an informational cascade with links to the filamentous fungi. *Microbiol. Mol. Biol. Rev.* 62:249–274.

Bibby, K. J., and C. A. McCulloch. 1994. Regulation of cell volume and $[Ca^{2+}]_i$ in attached human fibroblasts responding to anisosmotic buffers. *Am. J. Physiol. Cell Physiol.* 266:C1639–C1649.

Buckwalter, J. A. 1995. Aging and degeneration of the human intervertebral disk. *Spine.* 20:1307–1314.

Bush, P. G., and A. C. Hall 2001. The osmotic sensitivity of isolated and in situ bovine articular chondrocytes. *J. Orthop. Res.* 19:768–778.

Cantiello, H. F. 1997. Role of actin filament organization in cell volume and ion channel regulation. *J. Exp. Zool.* 279:425–435.

Colliou, O. K., J. R. Chin, E. C. Liebenberg, and J. C. Lotz. 1998. Matrix disorganization, apoptosis and gene expression in the intervertebral disk are modulated by compressive loading: a mouse model for disk degeneration. *Trans. Orthop. Res. Soc.* 23:189.

Dascalu, A., R. Korenstein, Y. Oron, and Z. Nevo. 1996. A hyperosmotic stimulus regulates intracellular pH, calcium, and S-100 protein levels in avian chondrocytes. *Biochem. Biophys. Res. Commun.* 227:368–373.

Dascalu, A., A. Matithyou, Y. Oron, and R. Korenstein. 2000. A hyperosmotic stimulus elevates intracellular calcium and inhibits proliferation of a human keratinocyte cell line. *J. Invest. Dermatol.* 115:714–718.

Engstrom, K. G., B. Moller, and H. J. Meiselman. 1992. Optical evaluation of red blood cell geometry using micropipette aspiration. *Blood Cells.* 18:241–257.

Erickson, G. R., L. G. Alexopoulos, and F. Guilak. 2001. Hyperosmotic stress induces volume change and calcium transients in chondrocytes by transmembrane, phospholipid, and G-protein pathways. *J. Biomech.* 34:1527–1535.

Errington, R. J., K. Puustjarvi, I. R. F. White, S. Roberts, and J. P. G. Urban. 1998. Characterization of cytoplasm-filled processes in cells of the intervertebral disk. *J. Anat.* 192:369–378.

Guilak, F., G. R. Erickson, and H. P. Ting-Beall. 2002. The effects of osmotic stress on the viscoelastic and physical properties of articular chondrocytes. *Biophys. J.* 82:720–727.

Guilak, F., H. P. Ting-Beall, A. E. Baer, W. R. Trickey, G. R. Erickson, and L. A. Setton. 1999. Viscoelastic properties of intervertebral disk cells. Identification of two biomechanically distinct cell populations. *Spine.* 24:2475–2483.

Guizouarn, H., R. Motais, F. Garcia Romeu, and F. Borgese. 2000. Cell volume regulation: the role of taurine loss in maintaining membrane potential and cell pH. *J. Physiol.* 523(Pt 1):147–154.

Hall, A. C., I. Starks, C. L. Shoults, and S. Rashidbigi. 1996. Pathways for K^+ transport across the bovine articular chondrocyte membrane and their sensitivity to cell volume. *Am. J. Physiol. Cell Physiol.* 270: C1300–C1310.

Hallows, K. R., F. Y. Law, C. H. Packman, and P. A. Knauf. 1996. Changes in cytoskeletal actin content, F-actin distribution, and surface morphology during HL-60 cell volume regulation. *J. Cell Physiol.* 167:60–71.

Hamilton, M. T., D. S. Ward, and P. D. Watson. 1993. Effect of plasma osmolality on steady-state fluid shifts in perfused cat skeletal muscle. *Am J. Physiol. Regulatory Integrative Comp. Physiol.* 265: R1318–R1323.

Hardingham, G. E., and H. Bading. 1999. Calcium as a versatile second messenger in the control of gene expression. *Microsc. Res. Tech.* 46: 348–355.

Henson, J. H. 1999. Relationships between the actin cytoskeleton and cell volume regulation. *Microsc. Res. Tech.* 47:155–162.

Hildebrandt, J. P., and A. Prowald. 2000. Ca(2+) and p38 MAP kinase regulate mAChR-mediated c-Fos expression in avian exocrine cells. *Am J. Physiol. Cell Physiol.* 278:C879–C884.

Hoffmann, E. K., and P. B. Dunham. 1995. Membrane mechanisms and intracellular signaling in cell volume regulation. *Int. Rev. Cytol.* 161: 173–262.

Ingber, D. E., L. Dike, L. Hansen, S. Karp, H. Liley, A. Maniotis, H. McNamee, D. Mooney, G. Plopper, and J. Sims. 1994. Cellular tensegrity: exploring how mechanical changes in the cytoskeleton regulate cell growth, migration, and tissue pattern during morphogenesis. *Int. Rev. Cytol.* 150:173–224.

Ishihara, H., H. Tsuji, N. Hirano, H. Ohshima, and N. Terahata. 1992. Effects of continuous quantitative vibration on rheologic and biological behaviors of the IVD. *Spine.* 17(Suppl):S7–S12.

Ishihara, H., K. Warensjo, S. Roberts, and J. P. Urban. 1997. Proteoglycan synthesis in the intervertebral disk nucleus: the role of extracellular osmolality. *Am J. Physiol. Cell Physiol.* 272:C1499–C1506.

Jones, W. R., G. M. Lee, S. S. Kelley, and F. Guilak. 1999. Viscoelastic properties of chondrocytes from normal and osteoarthritic human cartilage. *Trans. Orthop. Res. Soc.* 24:157.

Kajstura, J., and K. Reiss. 1989. F-actin organization influences the osmotic reactions of animal cells. *Folia Histochem. Cytobiol.* 27:201–208.

Kinosian, H. J., L. A. Selden, J. E. Estes, and L. C. Gershman. 1993. Actin filament annealing in the presence of ATP and phalloidin. *Biochemistry.* 32:12353–12357.

Lang, F., G. L. Busch, and H. Volkl. 1998. The diversity of volume regulatory mechanisms. *Cell Physiol. Biochem.* 8:1–45.

Lange, K. 1999. Microvillar Ca^{++} signaling: a new view of an old problem. *J. Cell Physiol.* 180:19–34.

Lange, K. 2000. Regulation of cell volume via microvillar ion channels. *J. Cell Physiol.* 185:21–35.

Lange, K., and U. Brandt. 1996. Calcium storage and release properties of F-actin: evidence for the involvement of F-actin in cellular calcium signaling. *FEBS Lett.* 395:137–142.

Le Bihan, T., and C. Gicquaud. 1991. Stabilization of actin by phalloidin: a differential scanning calorimetric study. *Biochem. Biophys. Res. Commun.* 181:542–547.

Lipp, P., and E. Niggli. 1993. Ratiometric confocal Ca(2+)-measurements with visible wavelength indicators in isolated cardiac myocytes. *Cell Calcium.* 14:359–372.

Maldonado, B. A., and T. R. Oegema. 1992. Initial characterization of the metabolism of intervertebral disk cells encapsulated in microspheres. *J. Orthop. Res.* 10:677–690.

Malko, J. A., W. C. Hutton, and W. A. Fajman. 1999. An in vivo magnetic resonance imaging study of changes in the volume (and fluid content) of the lumbar intervertebral disks during a simulated diurnal load cycle. *Spine.* 24:1015–1022.

Maximov, A. V., E. A. Vedernikova, H. Hinssen, S. Y. Khaitlina, and Y. A. Negulyaev. 1997. Ca-dependent regulation of Na+-selective channels via actin cytoskeleton modification in leukemia cells. *FEBS Lett.* 412:94–96.

McCarty, N. A., and R. G. O'Neil. 1992. Calcium signaling in cell volume regulation. *Physiol. Rev.* 72:1037–1061.

McMillan, D. W., G. Garbutt, and M. A. Adams. 1996. Effect of sustained loading on the water content of intervertebral disks: implications for disk metabolism. *Ann. Rheum. Dis.* 55:880–887.

Moustakas, A., P. A. Theodoropoulos, A. Gravanis, D. Haussinger, and C. Stournaras. 1998. The cytoskeleton in cell volume regulation. *Contrib. Nephrol.* 123:121–134.

Oegema, T. R. 1993. Biochemistry of the intervertebral disk. *Clin. Sports Med.* 12:419–439.

Ohshima, H., H. Tsuji, N. Hirano, H. Ishihara, Y. Katoh, and H. Yamada. 1989. Water diffusion pathway, swelling pressure, and biomechanical properties of the intervertebral disk during compression load. *Spine.* 14:1234–1244.

Ohshima, H., J. P. Urban, and D. H. Bergel. 1995. Effect of static load on matrix synthesis rates in the intervertebral disk measured in vitro by a new perfusion technique. *J. Orthop. Res.* 13:22–29.

O'Neill, W. C. 1999. Physiological significance of volume-regulatory transporters. *Am. J. Physiol. Cell Physiol.* 276:C995–C1011.

Paajanen, H., I. Lehto, A. Alanen, M. Erkintalo, and M. Komu. 1994. Diurnal fluid changes of lumbar disks measured indirectly by magnetic resonance imaging. *J. Orthop. Res.* 12:509–514.

Perlman, D. F., and L. Goldstein. 1999. Organic osmolyte channels in cell volume regulation in vertebrates. *J. Exp. Zool.* 283:725–733.

Ragette, R., C. Fu, and J. Bhattacharya. 1997. Barrier effects of hyperosmolar signaling in microvascular endothelium of rat lung. *J. Clin. Invest.* 100:685–692.

Rivero, F., B. Koppel, B. Peracino, S. Bozzaro, F. Siegert, C. J. Weijer, M. Schleicher, R. Albrecht, and A. A. Noegel. 1996. The role of the cortical cytoskeleton: F-actin crosslinking proteins protect against osmotic stress, ensure cell size, cell shape and motility, and contribute to phagocytosis and development. *J. Cell Sci.* 109(Pt. 11):2679–2691.

Rosado, J. A., and S. O. Sage. 2000. The actin cytoskeleton in store-mediated calcium entry. *J. Physiol.* 526(Pt 2):221–229.

Sato, M., D. P. Theret, L. T. Wheeler, N. Ohshima, and R. M. Nerem. 1990. Application of the micropipette technique to the measurement of cultured porcine aortic endothelial cell viscoelastic properties. *J. Biomech. Eng.* 112:263–268.

Schliess, F., R. Sinning, R. Fischer, C. Schmalenbach, and D. Haussinger. 1996. Calcium-dependent activation of Erk-1 and Erk-2 after hypo-osmotic astrocyte swelling. *Biochem. J.* 320(Pt. 1):167–171.

Schliwa, M. 1982. Action of cytochalasin D on cytoskeletal networks. *J. Cell Biol.* 92:79–91.

Sheikh, S., W. B. Gratzer, J. C. Pinder, and G. B. Nash. 1997. Actin polymerization regulates integrin-mediated adhesion as well as rigidity of neutrophils. *Biochem. Biophys. Res. Commun.* 238:910–915.

Small, J. V., and M. Gimona. 1998. The cytoskeleton of the vertebrate smooth muscle cell. *Acta Physiol. Scand.* 164:341–348.

Ting-Beall, H. P., A. S. Lee, and R. M. Hochmuth. 1995. Effect of cytochalasin D on the mechanical properties and morphology of passive human neutrophils. *Ann. Biomed. Eng.* 23:666–671.

Toribatake, Y., W. C. Hutton, W. A. Elmer, T. E. Whitesides, and K. Tomita. 1997. An in vivo study of the effect of applied compressive force on intervertebral disk metabolism. *Trans. Orthop. Res. Soc.* 22: 145.

Trickey, W., T. Vail, T. Wright, and F. Guilak. 2000. The role of the cytoskeleton in the viscoelastic properties of osteoarthritic human chondrocytes. *Trans. Orthop. Res. Soc.* 25:930.

Trout, J. J., J. A. Buckwalter, K. C. Moore, and S. K. Landas. 1982. Ultrastructure of the human intervertebral disk. I. Changes in notochordal cells with age. *Tissue Cell.* 14:359–369.

Tsai, M. A., R. S. Frank, and R. E. Waugh. 1994. Passive mechanical behavior of human neutrophils: effect of cytochalasin B. *Biophys. J.* 66:2166–2172.

Tseng, Y., E. Fedorov, J. M. McCaffery, S. C. Almo, and D. Wirtz. 2001. Micromechanics and ultrastructure of actin filament networks crosslinked by human fascin: a comparison with alpha-actinin. *J. Mol. Biol.* 310:351–366.

Urban, J. P., H. Ishihara, and M. J. Mouat. 1994. Differential metabolic responses of the nucleus and outer annulus to changes in extracellular physical factors. *Trans. Orthop. Res. Soc.* 19:134.

Verkman, A. S., A. N. van Hoek, T. Ma, A. Frigeri, W. R. Skach, A. Mitra, B. K. Tamarappoo, and J. Farinas. 1996. Water transport across mammalian cell membranes. *Am J. Physiol. Cell Physiol.* 270:C12–C30.

Waldegger, S., S. Steuer, T. Risler, A. Heidland, G. Capasso, S. Massry, and F. Lang. 1998. Mechanisms and clinical significance of cell volume regulation. *Nephrol. Dial. Transplant.* 13:867–874.

Wang, N. 1998. Mechanical interactions among cytoskeletal filaments. *Hypertension.* 32:162–165.

Wang, J. Y., A. E. Baer, V. B. Kraus, and L. A. Setton. 2001. Intervertebral disk cells exhibit differences in gene expression in alginate and monolayer culture. *Spine.* 26:1747–1752.

Warskulat, U., F. Schliess, and D. Haussinger. 1998. Compatible organic osmolytes and osmotic modulation of inducible nitric oxide synthetase in RAW 264.7 mouse macrophages. *Biol. Chem.* 379:867–874.

Wendel, H., and P. Dancker. 1987. Influence of phalloidin on both the nucleation and the elongation phase of actin polymerization. *Biochim. Biophys. Acta.* 915:199–204.

Wu, Z. Z., G. Zhang, M. Long, H. B. Wang, G. B. Song, and S. X. Cai. 2000. Comparison of the viscoelastic properties of normal hepatocytes and hepatocellular carcinoma cells under cytoskeletal perturbation. *Biorheology.* 37:279–290.